J Solid State Electrochem (2008) 12:315–322
DOI 10.1007/s10008-007-0393-2

ORIGINAL PAPER

Development of CeO_2- and TiO_2-incorporated aluminium metal-composite matrix with high resistance to corrosion and biofouling

P. Muhamed Ashraf · S. M. A. Shibli

Received: 15 January 2007 / Revised: 14 July 2007 / Accepted: 16 July 2007 / Published online: 10 August 2007

Abstract Cerium oxide (CeO_2) is a potential corrosion inhibitor for aluminium, and titanium oxide (TiO_2) is an efficient anti-fouling agent in the marine environment. The present study explored the possibility of incorporating CeO_2 and TiO_2 in aluminium to prepare a metal matrix composite that could have high corrosion and biofouling resistance under marine conditions. Such incorporation of CeO_2 and TiO_2 in pure aluminium offered high resistance to corrosion and biogrowth under marine conditions as evidenced during different tests. The specimens exhibited more anodic and stable open circuit potential throughout the period of the study. The optimum concentration of CeO_2 and TiO_2 was found to be 0.2 and 0.1%, respectively. The present results lay emphasis on the potential scope of the use of CeO_2- and TiO_2-incorporated aluminium in marine environments.

Keywords Cerium oxide · Titanium oxide · Marine corrosion · Corrosion control · Metal matrix composite · Biofouling

Introduction

Aluminium is extensively used as a good structural material because of its merits such as low cost, excellent strength-to-weight ratio and high resistance to corrosion [1]. Aluminium metal and alloys are reinforced with lightweight particles or fibres to form metal matrix composites (MMCs) to improve their physical and mechanical properties [2–4]. Aluminium is extensively used for preparing MMCs because of its low density, high strength and high ductility. Challis [5] in his review highlighted the scope of the use of aluminium composites in submarines, as it will reduce the hull weight leading to lower fuel consumption. Ceramic particles such as SiC and Al_2O_3 are extensively used for reinforcing aluminium and its alloys. SiO_2, ZrO_2 and TiB_2 have also been investigated for reinforcing aluminium [6]. Ceramic oxides have several advantages such as low thermal expansion and high fracture toughness [7]. Cerium oxide (CeO_2) can be considered for the preparation of MMCs, because of its merits like easy availability and high stability against mechanical abrasion, chemical attack and high temperature. CeO_2 is also one of the highly refractory oxides (melting point, 2,873 K) that posses a great oxygen storage capacity [8]. CeO_2 can be used efficiently for inhibition of Al, steel and Mg corrosion [9–11]. The authors have developed a MMC of pure aluminium reinforced with CeO_2 and reported that the matrix possessed excellent corrosion resistance under marine conditions [12].

Biofouling is a major observation next to corrosion in deteriorating metallic components in marine environments. Adhesion of bacteria on solid surface is governed by electrostatic, van der Waals and Lewis acid–base interactions. Both bacterial and solid surface properties such as solid surface roughness and hydrophobicity govern the initial adhesion phase of bacteria on the surface. Bacterial attachment and subsequent cell growth on the metal surface lead to biofouling and deterioration of metals [13]. The photo-induced biocidal characteristics of titanium oxide (TiO_2) have been studied extensively [14–17]. To incorporate TiO_2 in Al-based MMCs, TiO_2 is reduced to Ti, which then

P. M. Ashraf · S. M. A. Shibli (✉)
Department of Chemistry, University of Kerala,
Kariavattom Campus,
Trivandrum, Kerala, India 695 581
e-mail: smashibli@yahoo.com

forms an inter-metallic compound with Al in the MMCs [18, 19]. Aluminium and alloys such as Al–2Cu, Al–1Mg–0.6Si (6061), Al–4.5Cu, Al–10Mg and Al–7Si–0.6Mg (A357) are generally used for preparing MMCs [20]. Titanium coating on aluminium surface can suppress both corrosion and biofouling effectively [21]. As discussed above, CeO_2 is one of promising inhibitors of corrosion of aluminium in marine environments [12], whereas TiO_2 could be effectively used for the control of biofouling. In the present work, MMCs of CeO_2- and TiO_2-incorporated aluminium were fabricated, and their biofouling and corrosion resistance characteristics were studied.

Experimental

Electrolytic-grade pure aluminium (99.80%) ingots were used for the fabrication of MMCs. The aluminium ingots had the percentage composition (w/w) of Cu, Fe, Mg, Mn, Ti and Zn as 0.0031, 0.1069, 0.0411, 0.0024, 0.0001 and 0.0016, respectively, the rest being aluminium. There was no chromium and nickel. The ingots were melted at 800± 10 °C in a muffle furnace. The required amounts of CeO_2 AR (CDH, 99.9%) and TiO_2 AR (Qualigens, 99.9%) powders were pre-heated to 800±10 °C before being added into the melt and stirred using a SiC rod. The melt was again kept in the muffle furnace for another 15 min at the same temperature and poured into a red brick mould. The cast aluminium coupons were sliced into an appropriate shape and polished using a series of silicon carbide papers up to 600 grits. The coupons were cleaned in an ultrasound bath, wiped with acetone and rinsed with distilled water (MilliQ Gradient). Five batches of aluminium composites incorporated with different concentrations CeO_2 and TiO_2 was fabricated, and their concentrations are given in Table 1.

Electrochemical impedance spectroscopy (EIS), linear sweep voltammetry (LSV) and other electrochemical measurements were carried out using an electrochemical analyzer (Autolab PGSTAT 30 plus FRA 2). EIS analysis was carried out in 3.5% (v/v) NaCl as the electrolyte. Ag/AgCl, Pt and the coupon having a 1-cm^2 exposed area was used as reference, counter and working electrodes, respectively. The impedance analysis was carried out at the frequency range of 1 MHz to 0.1 Hz with reference to the open circuit potential (OCP) after 30 min of exposure of the coupon in the electrolyte. The coupon having a 1-cm^2 exposed area was immersed in 3.5% NaCl for 1 h before the potentiodynamic polarization experiment at a scan rate of 0.010 V s^{-1}. Potential sweep was carried out from cathodic to anodic region (±0.500 V from OCP). Weight loss measurements were made after exposing the pre-weighed coupons in 3.5% NaCl for a period of 40 days as per ASTM G31-72. All the above analyses were carried out with at least three replications. The coupons were cleaned using a hot solution of phosphoric acid (50 mL L^{-1}) and potassium dichromate (20 g L^{-1}). The coupons were rinsed with distilled water, dried and weighed. Another set of experiments was carried out in parallel, and the OCP of each coupon was monitored continuously for 40 days, washed with distilled water and subjected to EIS analysis to understand the changes in the impedance spectra because of the immersion in NaCl.

By applying an anodic current of 100 mA cm^{-2}, the surface layers of CeO_2–TiO_2-incorporated aluminium coupons were removed in 3.5% NaCl. Eight batches of the coupons were subjected to such anodic stripping process with different durations in multiples of hours. The stable OCP was recorded after each set of the process. Another set of the pre-weighed coupons were exposed to salt spray for 100 h as per ASTM B 117-73. The coupons removed after the test were cleaned using an aluminium pickling solution of phosphoric acid (50 mL L^{-1}) and potassium dichromate (20 g L^{-1}). The corrosion rates of the coupons were calculated as per ASTM G1-72. The surface of fresh CeO_2- and TiO_2-incorporated aluminium coupons were polished using a series of SiC papers up to 2,000 grit followed by etching with 1% (w/v) NaOH solution, and their scanning electron micrographs were recorded using a Hitachi scanning electron microscope at 15 keV.

The CeO_2- and TiO_2-incorporated aluminium coupons were immersed in Cochin estuary (Kerala, South India) for 2 days to evaluate the effect of the composite against microbial corrosion. Sterile cotton swabs were moistened with sterile phosphate buffer solution and swabbed a known surface area. One millilitre of phosphate buffer was plated with sterile tryptone glucose beef extract agar (15–20 mL per Petri plate). The agar was allowed to set for 30 min and then incubated at 37 °C for 48 h. Counts of the colonies formed on the plates were counted, and the colony-forming unit areas (cfu cm^{-2}) were calculated. The pure aluminium coupons were also exposed as the control.

Table 1 Concentrations of TiO_2 and CeO_2 incorporated in aluminium fabricated in different batches

Batch	Percentage of CeO_2	Percentage of TiO_2				
		0.05	0.10	0.20	0.40	0.70
A	0.00	A1	A2	A3	A4	A5
B	0.05	B1	B2	B3	B4	B5
C	0.10	C1	C2	C3	C4	C5
D	0.20	D1	D2	D3	D4	D5
E	0.40	E1	E2	E3	E4	E5

The term B3 designates the aluminium composite incorporated with 0.05% CeO_2 and 0.20% TiO_2

Results and discussion

Effect of CeO_2 and TiO_2

Our previous studies revealed that the incorporation of CeO_2 in pure aluminium could reduce the corrosion of aluminium in marine environments [12]. Preliminary tests were conducted to study the effect of the incorporation of mixed oxides viz. TiO_2 and CeO_2 in aluminium. The incorporation of TiO_2 along with CeO_2 in aluminium was to improve the electrochemical parameters. To optimize the concentration of TiO_2 to be incorporated, a series of TiO_2-incorporated aluminium was fabricated and studied. Different concentration of TiO_2-incorporated coupons viz. 0.05, 0.10, 0.20, 0.40 and 0.70% (w/w) were prepared and designated as batch A. The coupons were subjected to LSV. The *i* vs *E* plots are shown in Fig. 1. The values of E_{corr}, I_{corr}, R_p and corrosion rate obtained from the voltammogram was varied from −0.691 to −0.783 V, 7.53×10^{-7} to 3.06×10^{-6} A cm^{-2}, 4,550 to 28,800 Ω and 0.3404 to 1.324 mpy, respectively. The E_{corr}, I_{corr}, R_p and the corrosion rate of pure aluminium were found to be −0.681 V, 1.13×10^{-6} A cm^{-2}, $8.19\times10^{+3}$ Ω and 0.492 mpy, respectively. The 0.40% TiO_2-incorporated aluminium coupons exhibited the highest polarization resistance and lower corrosion rate. Higher amounts of TiO_2 concentration in aluminium did not proportionally improve the LSV parameters. Hence, the concentration of TiO_2 in aluminium should be less than 0.4%. Based on the above information, four batches of CeO_2- and TiO_2-incorporated aluminium coupons were fabricated, and it was designated by letters B, C, D and E. The compositions of CeO_2 and TiO_2 in other aluminium coupons are shown in Table 1.

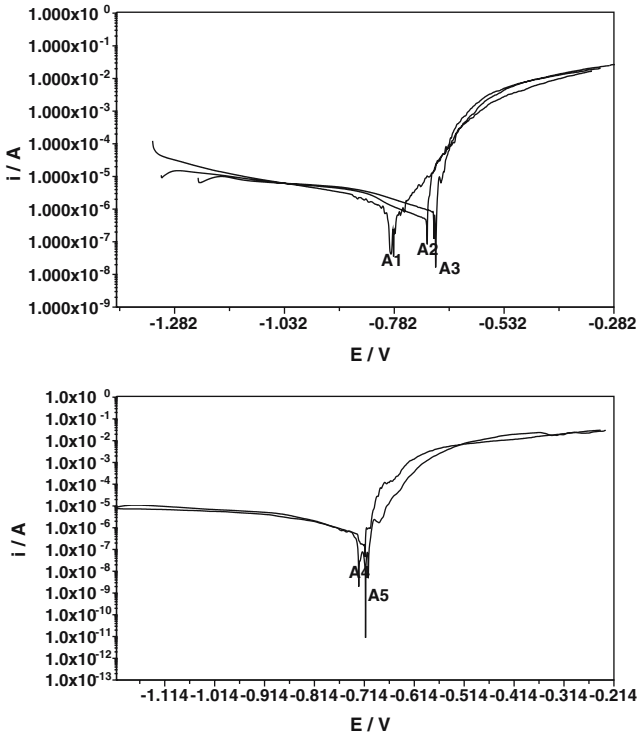

Fig. 1 The *i* vs *E* plots of TiO_2-incorporated aluminium, where *A1* 0.05% TiO_2, *A2* 0.10% TiO_2, *A3* 0.20% TiO_2, *A4* 0.40% TiO_2 and *A5* 0.70% TiO_2

The aluminium composites fabricated in different batches were subjected to electrochemical tests like impedance analysis, LSV, weight loss and salt spray tests, and their mean values were shown in Table 2. Linear polarization parameters E_{corr}, I_{corr}, R_p, corrosion rate and E_{pit} varied from −0.691 to −0.845 V, 1.71×10^{-7} to 8.71×10^{-6} A cm^{-2}, 4,550 to 54,455 Ω, 0.072 to 3.136 mpy and −0.704 to −0.920 V, respectively. The CeO_2- and TiO_2-incorporated aluminium coupons exhibited a significant reduction in the pitting potential (E_{pit}). The R_p, constant phase element (CPE) and *n* (empirical constant related to CPE) values in the high frequency region of impedance spectra were found to be in the range from 46.41 to 89.36 Ω, 6.31×10^{-9} to 1.32×10^{-8} F and 1.16 to 1.32, respectively. The batch D aluminium coupons incorporated with 0.20% CeO_2 plus varying amounts of TiO_2 exhibited highest corrosion resistance when compared to other batches of the aluminium composites (Table 2). In this context, the paper restricts the discussion only to the batch D coupons, viz. D1 (Al+0.2% CeO_2+0.05% TiO_2), D2 (Al+0.2% CeO_2+0.10% TiO_2), D3 (Al+0.2% CeO_2+0.20% TiO_2) and D4 (Al+0.2% CeO_2+0.40% TiO_2).

Synergistic effect of CeO_2 and TiO_2

Impedance studies

All the coupons of the D batch were subjected to electrochemical impedance spectroscopic analysis. A wider semicircle at the high-frequency region of the Nyquist plot was observed for the aluminium incorporated with CeO_2 and TiO_2 compared to the aluminium incorporated with TiO_2 alone (Fig. 2). The phase angle, R_p, CPE and *n* in the high-frequency region of the impedance spectrum were found to be in the range of 63.31–76.10°, 84.7–89.36 Ω, 1.16×10^{-8}–1.28×10^{-8} F and 1.31–1.35, respectively. The higher polarization resistance of the CeO_2- and TiO_2-incorporated aluminium coupons compared to the TiO_2-alone-incorporated aluminium, revealed an improvement in the corrosion resistance of the surface and inner layers. This is due to the incorporation of the mixed oxides and subsequent passivation. The mixed oxides kept the surface of the coupons less reactive as revealed based on higher polarization resistance and lower corrosion rate. An inductance-type impedance curve was exhibited in the case of the coupons incorporated with TiO_2 and CeO_2. The inductance

Table 2 The average and standard deviation data of linear sweep voltammetric analysis and determination of corrosion rate by different methods

Batch	Linear sweep voltammetry			Corrosion rate (mpy×10^{-4}) by weight loss	Corrosion rate (mpy×10^{-3}) by salt spray	E_{pit} (V)
	E_{corr} (V)	I_{corr} (A cm^{-2})	R_p (Ω)			
A	−0.728±0.037	$1.41\times10^{-6}\pm9.62\times10^{-7}$	16140±11135	4.806±1.17	3.647±1.31	−0.754±0.04
B	−0.714±0.022	$3.46\times10^{-6}\pm4.57\times10^{-6}$	10698±6760	8.857±3.25	2.761±1.46	−0.729±0.01
C	−0.742±0.071	$1.81\times10^{-6}\pm1.31\times10^{-6}$	15526±8831	8.570±2.86	3.461±1.03	−0.795±0.10
D	−0.734±0.036	$1.71\times10^{-6}\pm1.21\times10^{-6}$	22982±21406	4.22±3.37	2.495±0.72	−0.767±0.04
E	−0.758±0.057	$2.58\times10^{-6}\pm3.3\times10^{-6}$	23911±15353	5.647±1.24	1.476±0.56	−0.778±0.04

A TiO_2 0.05–0.7%, *B* 0.05% CeO_2+varied amounts of TiO_2 (0.05–0.4%), *C* 0.10%CeO_2+TiO_2 (0.05–0.4%), *D* 0.20% CeO_2+TiO_2 (0.05–0.4%), *E* 0.40%CeO_2+TiO_2 (0.05–0.4%)

loop was not clearly formed in the case of TiO_2-incorporated aluminium, whereas it was distinct for those coupons incorporated with TiO_2 and CeO_2. This revealed that the presence of CeO_2 along with TiO_2 in the aluminium matrix influenced the formation of an inductance curve. Based on their experiment with TiO_2-doped sensors, Santana et al. [22] reported that there was an inductance in the beginning of the high-frequency region of the corresponding Nyquisit plot. In the present study, the inductance was recorded at the end of the first semi-circle of the high-frequency region. This could be attributed to the synergistic action of TiO_2 and CeO_2 present in the inner layer of the matrix. Da Silva et al. [23] interpreted the main cause of such inductive behaviour to the disorderly movement of charge carriers through the complex microstructures comprising pores, cracks, grain boundaries etc. of the metal oxides-incorporated matrix. The origin of the distorted semi-circle in the low-frequency region could be attributed to the solid-state surface reduction–oxidation transitions, which is a faradaic process controlled by proton diffusion through the complex microstructure of the matrix (e.g. pores, cracks), associated to the influence of pore dimension and penetration depth of ac signal into the pores distributed along the rugged surface [24]. Therefore, the ac perturbation reaches the bottom of the pores containing the aluminium oxide, CeO_2 and TiO_2 layer only at lower frequencies. In that low-frequency domain, the impedance spectra could be characterized by a straight line presenting a phase angle greater than 90°. Such result revealed a pure capacitive behaviour of the oxide/solution interface.

Potentiodynamic polarization

Linear polarization analysis data of CeO_2- and TiO_2-incorporated aluminium (batch D) are shown in Table 3. Incorporation of TiO_2 along with CeO_2 in aluminium resulted in an increase in R_p and a decrease in I_{corr}. The 0.20% CeO_2- and 0.10% TiO_2-incorporated aluminium (sample D2) exhibited significantly high polarization resistance and low corrosion rate. The coupons D2 and D3 exhibited a passive range ($E_{corr}-E_{pit}$) at above 50 mV. Acceleration of the cathodic reaction and shifting of corrosion potential towards the passive region was achieved mainly by the addition of CeO_2. The formation of a passive film in the presence of two kinds of passivating elemental cations became highly stable than the surface film formed by a single component [25].

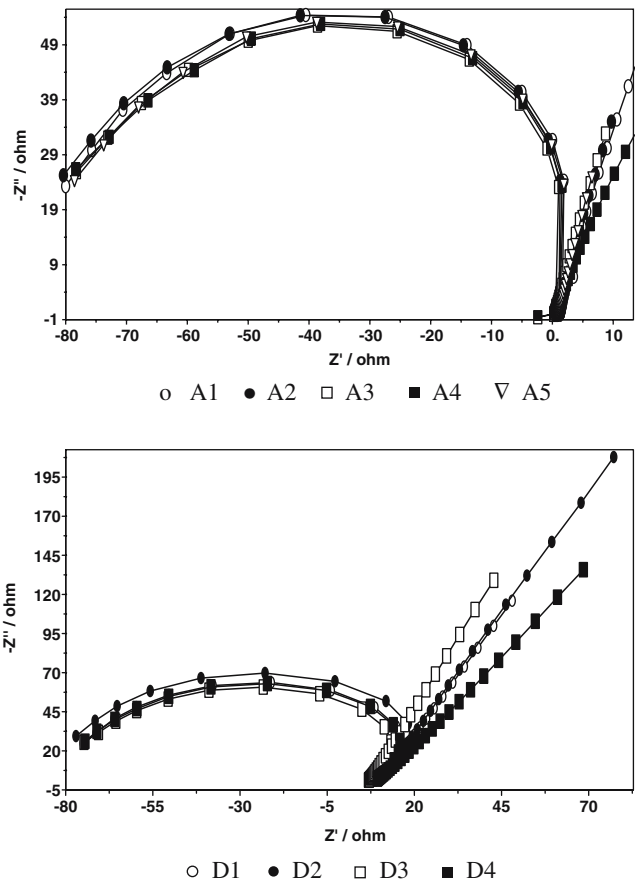

Fig. 2 The Nyquisit plots of fresh aluminium coupons incorporated with TiO_2 and TiO_2+CeO_2 in 3.5%NaCl at 30±1 °C, where *A1* 0.05% TiO_2 in Al, *A2* 0.10% TiO_2 in Al, *A3* 0.20% TiO_2 in Al, *A4* 0.40% TiO_2 in Al, *A5* 0.70% TiO_2 in Al. *D1* 0.2%CeO_2+0.05% TiO_2 in Al, *D2* 0.2%CeO_2+0.10% TiO_2 in Al, *D3* 0.2%CeO_2+0.20% TiO_2 in Al and *D4* 0.2%CeO_2+0.40% TiO_2 in Al

Table 3 The linear sweep voltammetric analysis parameters and corrosion rate (mpy) of the aluminium composites by weight loss method and salt spray test

Aluminium composite	E_{corr} (V)	I_{corr} (A cm^{-2})	R_p (Ω)	E_{pit} (V)	Corrosion rate (mpy) by weight loss	Corrosion rate (mpy) by salt spray
D1 (Al+0.2%CeO_2+0.05% TiO_2)	−0.763	2.76×10^{-6}	14528	−0.769	4.28×10^{-4}	3.00×10^{-3}
D2 (Al+0.20% CeO_2+0.10% TiO_2)	−0.767	4.87×10^{-7}	54455	−0.820	0.80×10^{-4}	1.46×10^{-3}
D3 (Al+0.20%CeO_2+0.20% TiO_2)	−0.702	8.46×10^{-7}	16360	−0.758	2.99×10^{-4}	2.55×10^{-3}
D4 (Al+0.20%CeO_2+0.40% TiO_2)	−0.703	2.73×10^{-6}	6585	−0.720	8.81×10^{-4}	2.98×10^{-3}
Al+0.10%TiO_2 incorporated Al	−0.707	9.05×10^{-7}	4550	−0.711	3.09×10^{-4}	2.18×10^{-3}
Pure Al	−0.681	1.13×10^{-6}	8190	−0.695	75.6×10^{-4}	2.07×10^{-3}

OCP decay and corrosion rate

The variation in OCP, as a function of time, of the 'D' batch coupons along with 0.2% CeO_2- and 0.10% TiO_2-incorporated aluminium immersed in 3.5% NaCl for a period of 40 days are illustrated in Fig. 3. After 2 days of immersion, the OCP of the CeO_2- and TiO_2-incorporated coupons slowly shifted towards a more cathodic region. Lower OCP was recorded for most of the coupons initially. Later, OCP of the coupons shifted towards a more cathodic potential, depending on the concentration of CeO_2 and TiO_2 in the matrix. The coupons incorporated with TiO_2 and CeO_2 exhibited a shift in OCP by less than −0.800 V within 2–5 days of its immersion in 3.5% NaCl. The coupons exhibited exceptionally stable OCP throughout the study period. The corrosion resistance of the composite as determined by the weight loss method revealed that the coupons incorporated with 0.20% CeO_2 and 0.10% TiO_2 had a significantly lower corrosion rate than the pure aluminium and the TiO_2-incorporated aluminium (Table 3). Corrosion inhibition efficiency was found to be more than 95% when compared to pure aluminium. The corrosion resistance under aggressive conditions was assessed by the salt spray test. The corrosion rate of the coupons varied from 0.0008 to 0.0053 mpy.

Delayed passivation

During the previous studies, the CeO_2-reinforced aluminium coupons exhibited a long anodic branch after the corrosion potential (E_{corr}) during linear polarization [12]. Figure 4 shows the E vs i plot of fresh and corroded aluminium incorporated with 0.20% CeO_2 and 0.10% TiO_2. Only the voltammogram of D2 is given in the figure for better understanding. The long anodic branch after E_{corr} was absent in the case of fresh CeO_2- and TiO_2-incorporated aluminium coupons. However, during long-term OCP decay, evaluation of these coupons in 3.5% NaCl exhibited an exceptional stability in OCP (Fig. 3). Linear polarization analysis was carried out again in batch D coupons after immersing in 3.5% NaCl for 40 days to understand the corrosion behaviour of the corroded coupons. All the coupons exhibited very

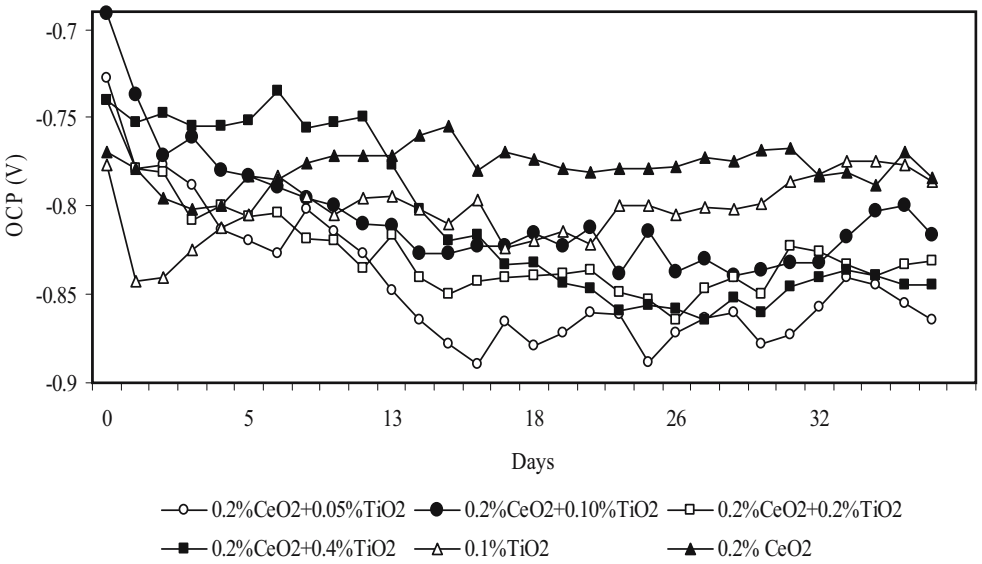

Fig. 3 The variation of open circuit potential of aluminium incorporated with CeO_2, TiO_2 and a mixture of CeO_2 plus TiO_2 during 40 days of immersion in 3.5% NaCl at 30±1 °C

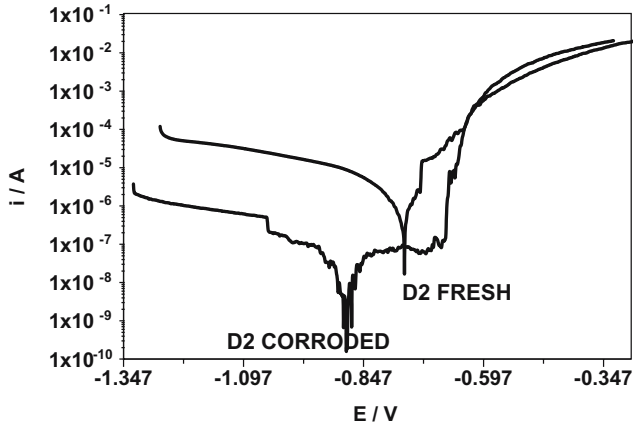

Fig. 4 The *i* vs *E* plots of CeO_2- (0.20%) and TiO_2- (0.10%) incorporated aluminium. Well-developed anodic branch after E_{corr} shown in aluminium coupons after 40 days of immersion in 3.5% NaCl

low E_{corr}, high R_p and a stable anodic branch of the polarization curve. Incorporation of CeO_2 in aluminium was responsible for the displacement of the cathodic branch towards lower current densities causing a decrease in the corrosion potential of the system. The corrosion rate of the coupons was reduced significantly because of the reduction in the cathodic sites in the matrix [26]. The shifting of corrosion potential towards more cathodic region could be attributed to the property of the cerium ions that acted as cathodic inhibitors against uniform and localized corrosion. This could be attributed to the suppression of the oxygen reduction reaction.

Structural evaluation

The presence of TiO_2 in aluminium caused improvement in brightness of the surface even after long-term immersion tests in aggressive environments. There was no blackening

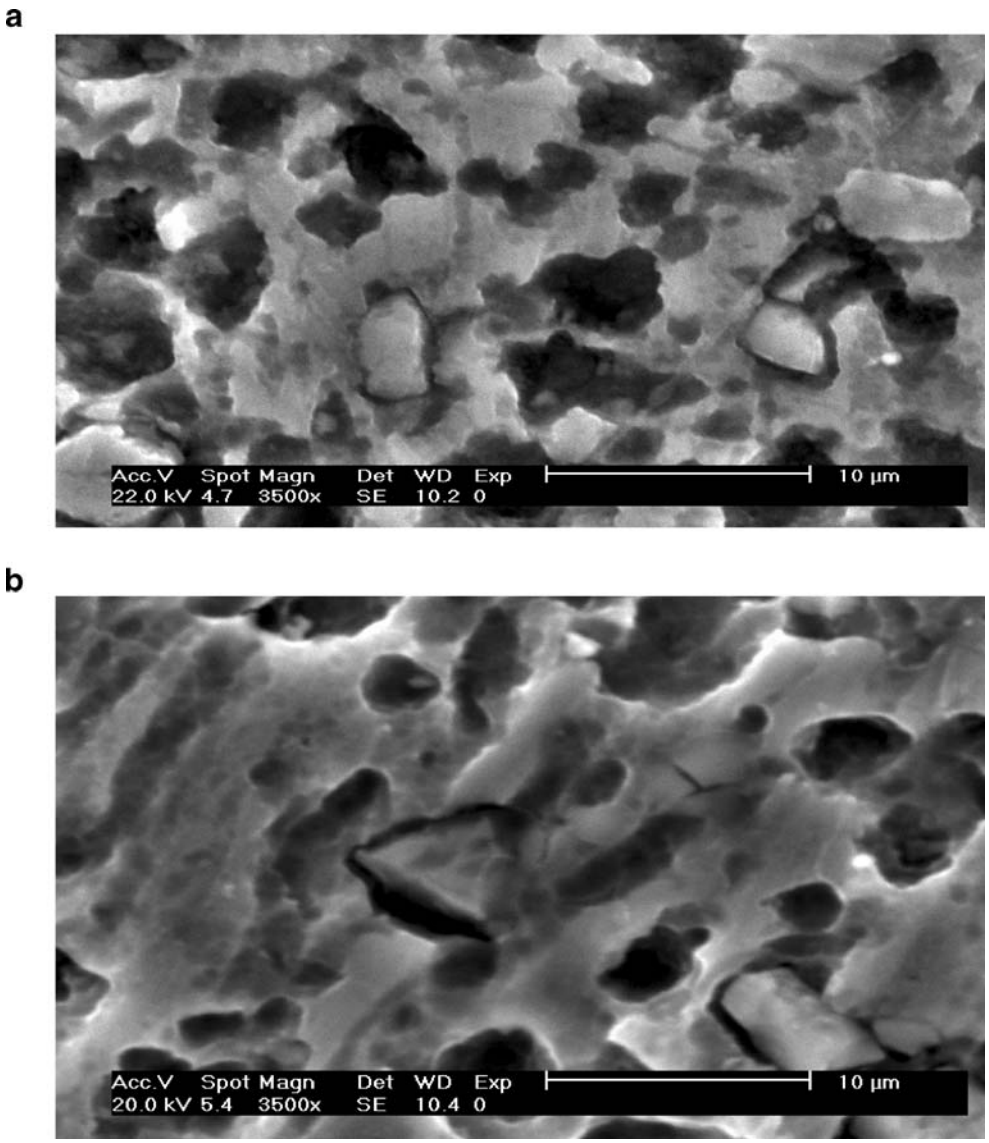

Fig. 5 The SEM micrographs of surfaces different aluminium coupons incorporated with **a** TiO_2 and **b** mixed oxides of both CeO_2 and TiO_2

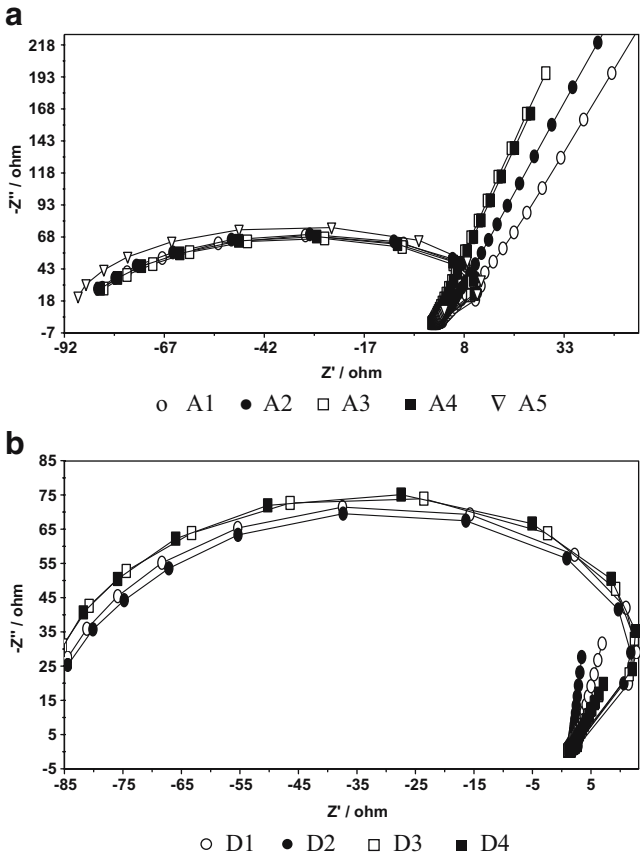

Fig. 6 The Nyquisit plots of aluminium coupons incorporated with **a** TiO_2 and **b** CeO_2+TiO_2 after subjecting to immersion 3.5% NaCl at 30±1 °C, where *A1* 0.05% TiO_2 in Al, *A2* 0.10% TiO_2 in Al, *A3* 0.20% TiO_2 in Al, *A4* 0.40% TiO_2 in Al, *A5* 0.70% TiO_2 in Al. *D1* 0.20% CeO_2+0.05% TiO_2 in Al, *D2* 0.20% CeO_2+0.10% TiO_2 in Al, *D3* 0.20% CeO_2+0.20% TiO_2 in Al and *D4* 0.20% CeO_2+0.40% TiO_2 in Al

because of aluminium oxide formation on the surface emphasizing the improvement of material and economic values. The coupons were subjected to anodic stripping by applying an anodic current of 100 mA cm^{-2}. After every multiple of 1-h intervals of current interruption, the OCP of the freshly exposed surface was monitored. The process was repeated for eight batches (8 h). An average OCP of −0.773±0.047 to −0.817±0.060 V was observed in the case of TiO_2- and CeO_2-incorporated aluminium, which revealed that the TiO_2 and CeO_2 composites were uniformly distributed in aluminium. Heterogeneity in the inner layers, if any, could cause a high difference in the potential values. Scanning electron micrographs also revealed that the TiO_2 and CeO_2 were distributed in the matrix uniformly. Both TiO_2 and CeO_2 were embedded closely in the matrix (Fig. 5). The micrographs revealed a void and defect-free surface of the aluminium matrix, which was amorphous in nature. There was an improvement in size and uniformity of the grains because of CeO_2 addition. Small grain size and their uniform distribution are normally predicted to yield high coloumbic efficiency in the sacrificial anodes. In short, the surface characteristics were improved because of the incorporation of TiO_2 and CeO_2.

Extended evaluation

EIS analysis was carried out after immersing the coupons in 3.5% NaCl for 40 days as shown in Fig. 6. The spectra exhibited that the radius of the semi-circle formed in the high frequency range of the Nyquisit plot was reduced significantly in the case of the TiO_2-incorporated Al coupons. The mixed CeO_2- and TiO_2-incorporated aluminium coupons exhibited a wider semi-circle and hence a higher polarization resistance in the high frequency region compared to the fresh coupons. The R_p value of the TiO_2-incorporated aluminium was in the range from 81.82 to 84.26 Ω, whereas it was 83.82–89.05 Ω for those coupons incorporated with CeO_2 and TiO_2. The phase angle of the CeO_2- and TiO_2-incorporated aluminium increased significantly. These results revealed that the effective passivation and high stability of the outer layer was achieved because of the presence of TiO_2 and CeO_2 in aluminium.

Biogrowth

TiO_2 (~3.5 eV) and CeO_2 (~5.5 eV) have comparable band gaps, and these composites can have a synergistic effect in resisting biofouling on the metal surface in marine environments. Such synergistic action resulting in a shift of electronic absorption to higher wavelength regions have also been reported in the case of TiO_2-incorporated Zn coating [27]. The photo-catalytic activity of TiO_2 can be significantly enhanced by the introduction of CeO_2 having four f electrons because the lanthanide ion can form complexes with various Lewis bases [28]. The photo-catalytic property of CeO_2 is significant because of (1) the presence of redox couple Ce^{3+}/Ce^{4+} in which CeO_2 exists as CeO_2 and Ce_2O_3

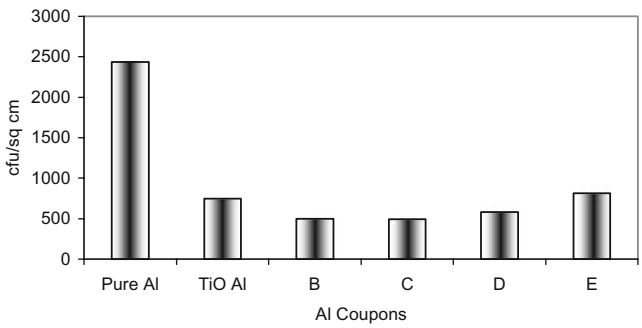

Fig. 7 The extent of microbial load (cfu cm^{-2}) on different aluminium coupons as a result of their exposure in the Cochin estuary. The coupon *B* is Al+0.05% CeO_2+0.10% TiO_2, *C* is Al+0.10% CeO_2+0.10% TiO_2, *D* is Al+0.20% CeO_2+0.10% TiO_2 and *E* is Al+0.40% CeO_2+0.10% TiO_2

depending on an oxidizing or a reducing condition and (2) the easy formation of labile oxygen vacancies with the relatively highly mobile bulk oxygen species [29].

To evaluate the anti-fouling effect, the coupons incorporated with 0.10% TiO_2 and different concentrations of CeO_2 viz. 0.05, 0.10, 0.2 or 0.4% were tested by immersing into the Cochin estuary. Microbial load in CeO_2- and TiO_2-incorporated aluminium, TiO_2-alone-incorporated aluminium and pure aluminium is shown in Fig. 7. The results exhibited a significant decrease in the microbial accumulation on the TiO_2-incorporated aluminium when compared with pure aluminium. A still more reduction in microbial concentration was observed on the coupons incorporated with CeO_2 and TiO_2. The substantially reduced number of microorganisms on the TiO_2 and CeO_2+TiO_2-incorporated coupons indicated a high biocidal nature of the TiO_2. The CeO_2 incorporation along with TiO_2 sharpened the biocidal activity of the latter. The probable mechanism could be that the Ce ion acted as an effective scavenger to trap the conduction band (CB) electron of TiO_2. The Ce ions, acting as a Lewis acid, apparently were superior to the oxygen molecule in terms of the capability of trapping CB electrons [30, 31]. The electron trapped in the Ce^{4+} /Ce^{3+} site was subsequently transferred to the surrounding adsorbed oxygen. The CB electrons reduced O_2 to the O_2^- radical, and it became H_2O_2 on further reduction. The presence of Ce^{4+} in the matrix might promote the formation of O_2^- and then with H^+ to form $OH^\bullet$ radicals. CeO_2 has a high oxygen transport and storage capacity [31]. The combination of the hydroxyl radicals themselves also could produce hydrogen peroxide. The hydroxyl radical and hydrogen peroxide are responsible for the biocidal effect. According to Garner and Heppel [32], because of the greater charge to volume ratios and despite their different valencies, all the lanthanides readily displace calcium from biological systems, and this will inhibit microbial activity.

Conclusion

The corrosion and biofouling of aluminium in marine environment can be suppressed efficiently by means of incorporating TiO_2 and CeO_2 in aluminium. The results of the present physicochemical, structural and electrochemical evaluation clearly revealed the effective role of TiO_2 and CeO_2 incorporation in aluminium exploring its use in marine environments. The best aluminium MMC prepared with an optimum concentration of 0.20% CeO_2 and 0.10% TiO_2 performed excellently. Incorporation of TiO_2 in the composite also improved brightness of the surface, indicating its commercial importance also. Significant reduction in microbial concentration in marine environments indicated that the composite could be a promising potential future for marine use.

Acknowledgements The authors sincerely thank the Director Dr. K Devadasan and Dr. B. Meenakumari, Head, Fishing Technology Division, Central Institute of Fishing Technology, for providing facilities to carry out the research work. Authors also thank Dr. Sanjeev S R, Principal Scientist, CIFT, for his help during microbiological evaluation of the composites.

References

1. Johnson BY, Edington J, O'Keefe MJ (2003) Mater Sci Eng A361:A225
2. Hooker JA, Doorbar PJ (2000) Mater Sci Tech 16:725
3. Kashyap KT, Ramachandra C, Datta C, Chatterjee B (2000) Bull Mater Sci 23:47
4. Cadek J, Kucharova K, Milicka K, Zhu S (1999) Metal Mater 37:213
5. Challis K (2001) Compos Struct 53:21
6. Torralba JM, da Costab CE, Velasco F (2003) J Mater Process Technol 133:203
7. Rosso M, Scrivani A, Ugues D, Bertini S (2001) Int J Refract Met Hard Mater 19:45
8. Murota T, Hasegawa T, Aozasa S, Matsui H, Motoyama M (1993) J Alloys Compd 193:298
9. Hinton BRW, Arnott DR, Ryan NE (1986) Mater Forum 9:162
10. Ardelean H, Fiaud C, Marcus P (2001) Mater Corros 52:889
11. Davenport AJ, Isaacs HS, Kendig MW (1991) Corros Sci 32:653
12. Ashraf PM, Shibli SMA (2007) Electrochem Comm 9:443
13. Li B, Logan BE (2005) Colloids Surf B Biointerfaces 41:153
14. Pin-Ching M, Sharon S, Daniel MB, Zheng H, Edward JW, William AJ (1999) Appl Environ Microbiol 59:4094
15. Byunghoon K, Dohwan K, Donglyun C, Sungyong C (2003) Chemosphere 52:277
16. William AJ, Pin-Ching M, Edward JW, Daniel MB, John AF (1998) Environ Sci Technol 32:2650
17. Shibli SMA, Dilimon VS, Antony SP, Manu R (2006) Surf Coat Technol 200:4791
18. Travitzky N, Gotman I, Claussen N (2003) Mater Lett 57:3422
19. Dong Q, Tang Q, Li WC, Wu DY (2002) Mater Lett 55:259
20. Vassel A (1999) Mater Sci Eng A 263:305
21. Sun Y (2004) Mater Lett 58:2635
22. Santana MHP, Da Silva LM, De Faria LA (2003) Electrochim Acta 48:1885
23. Da Silva LM, Fernandes KC, Da Faria LA, Boodts JFC (2004) Electrochim Acta 49:4893
24. Song HK, Hwang HY, Lee KH, Dao LH (2000) Electrochim Acta 45:2241
25. Akiyama E, Habazaki H, Kawashima A, Asami K, Hashimoto K (1997) Mater Sci Eng A 226–228:920
26. Kasten LS, Grant JT, Grabasch N, Yoevodin N, Arnold FE, Donley MS (2001) Surf Coat Technol 140:11
27. Deguchi T, Imai K, Matsui H, Iwasaki M, Tada H, Ito S (2001) J Mat Sci 36:4723
28. Li FB, Li XZ, Hou MF, Cheah KW, Choy WCH (2005) Appl Catal A Gen 285:181
29. Reddy BM, Sreekanth PM, Reddy EP, Yamada Y, Xu Q, Sakurai H, Kobayashi T (2002) J Phys Chem B 106:5695
30. Coronado JM, Maria AJ, Martínez-Arias A, Conesa JC, Soria J (2000) J Photochem Photobiol A Chem 150:213
31. Xie YB, Yuan CW (2003) Appl Catal B Environ 46:251
32. Garner JP, Heppel PSJ (2005) Burns 31:539